Algorithm for retrieving lidar ratios at 1064 nm from space-based lidar backscatter data

Mark Vaughan*
SAIC, Mail Stop 435, NASA Langley Research Center, Hampton VA, USA 23681- 2199

ABSTRACT

Accurate estimation of cloud and aerosol optical depths using backscatter lidar data requires knowledge of the particulate *lidar ratio* (i.e., the extinction-to-backscatter ratio). In those cases for which a measurement of molecular backscatter can be made on the far side of a layer, knowledge of the lidar ratio can be derived directly from the data. However, obtaining a reliable clear air constraint is a function of layer optical depth, system sensitivity and overall signal-to-noise ratio (SNR). To date, the design constraints imposed on space-based lidars such as LITE and CALIPSO have rendered the use of this retrieval technique virtually impossible for measurements made at 1064 nm.

Layers to which the constraint method can be successfully applied are assumed to be homogeneous with respect to particle composition and size distribution, and therefore are characterized by lidar ratios that are range-invariant throughout the layer. By extending this assumption of homogeneity to include the layer backscatter color ratio, this work derives a new technique that simultaneously retrieves both the color ratio and the 1064 nm lidar ratio from two wavelength elastic backscatter lidar measurements of transmissive clouds and/or lofted aerosol layers. Retrieval examples are illustrated using data obtained from LITE. Initial error estimates derived from numerical experiments using simulated data show the retrieval of the backscatter color ratio to be stable, even in the presence of considerable noise in the data.

Keywords: lidar, lidar ratio, extinction, algorithm

1. INTRODUCTION

The vertical profiling capability of space-based lidars promises to deliver a unique and valuable set of atmospheric measurements. The primary science data products extracted from these measurements are the base and top altitudes of clouds and aerosol layers and the associated range-resolved profiles of volume backscatter and extinction coefficients. Deriving these optical properties from the raw measurements requires an estimate of the lidar ratio, S, a quantity that depends both on the particulate scattering medium being sampled and on the laser wavelength employed for the measurement. To date, all space-based lidar measurements have been made at Nd:YAG wavelengths. The Lidar In-space Technology Experiment (LITE)[1] used the fundamental, doubled, and tripled outputs of an Nd:YAG laser – i.e., 1064 nm, 532 nm, and 355 nm, respectively – while the Geoscience Laser Altimeter System (GLAS)[2] currently makes atmospheric measurements using the 1064 nm and 532 nm wavelengths. Similarly, when the Cloud-Aerosol Lidar and Infrared Pathfinder Satellite Observations mission (CALIPSO)[3] launches in early 2005, it too will deploy an Nd:YAG-based lidar system. It follows therefore that the quality of the optical properties estimates delivered by these systems depends directly on the degree of accuracy with which we can derive or specify the lidar ratios at the Nd:YAG wavelengths.

When a reliable measurement of molecular attenuated backscatter can be made both above the layer top and beneath the layer base, the layer two-way transmittance can be estimated from the lidar data alone, and the requisite lidar ratio can be retrieved directly from the lidar measurements.[4] This procedure works well when using data acquired at the shorter YAG wavelengths. However, due to the reduced sensitivity to molecular backscatter at 1064 nm, and to the design restrictions imposed on the current generation of space-based lidars, this "lofted layer technique" cannot be used to retrieve lidar ratios from measurements made at 1064 nm. (Note that this is a practical restriction imposed by the restrictions of space flight, and not a fundamental limitation of the measurement technique.) A typical example of the spectral sensitivity differences is illustrated in Figure 1. Figure 1(a) shows a cirrus cloud measured at 532 nm during

* m.a.vaughan@larc.nasa.gov; phone 1 757 864 5331; fax 1 757 864 7775

Laser Radar Technology for Remote Sensing, edited by Christian Werner,
Proceedings of SPIE Vol. 5240 (SPIE, Bellingham, WA, 2004)
0277-786X/04/$15 · doi: 10.1117/12.510770

LITE orbit 141. When measured at 532 nm this feature qualifies as a transmissive cloud to which the lofted layer technique can be successfully applied: regions of molecular backscatter are available both above the layer top and below the layer base, with more than adequate signal-to-noise ratios (SNR) in both regions. In contrast, the companion measurement made at 1064 nm (see Figure 1(b)) shows no evidence of a clear air return anywhere within the profile. Therefore, the appropriate lidar ratio for the 1064 nm analysis must be obtained via means other than application of the lofted layer technique.

When lidar ratios cannot be obtained using the lofted layer technique, they must be specified using theoretical justifications and/or empirical heuristics. In the case of surface-attached aerosol layers, lidar ratios used in the analysis of space-based measurements are typically specified based on geography, season, and the accumulated knowledge of the scattering properties of locally likely aerosol types.[5,6] This approach has the potential for working quite well for measurements made using the second and third harmonics of a YAG laser, as several databases of S_{355} and S_{532} measurements have been compiled using Raman lidar[7,8], and a relatively large number of S_{550} measurements have been made using backscatter nephelometers.[9] However, even in the well-sampled regions of the planet (e.g., Europe, via EARLINET), the prognosis for the geographical/seasonal database technique at 1064 nm is substantially less encouraging, as reported measurements of S_{1064} are extremely sparse.

Figure 1: LITE background-subtracted raw data at (a) 532 nm and (b) 1064 nm showing a transmissive cirrus cloud (optical depth = 0.25) measured during orbit 141 at 12.98º North and 133.22º West. The profiles shown have been averaged to a 5-km horizontal resolution (7 laser pulses) and smoothed by 45 meters (3 range bins) vertically.

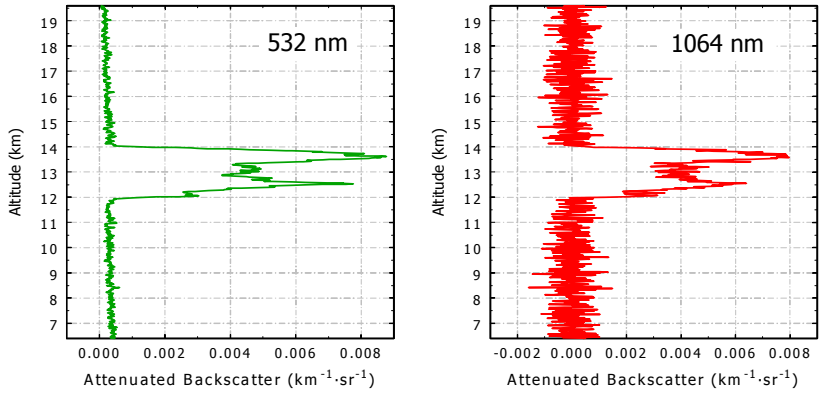

In this work I address the paucity of S_{1064} measurements by introducing a new technique for retrieving lidar ratios at 1064 nm. With respect to solving the lidar equation, two specific assumptions are made regarding the optical properties of the layers to which this method is applied.

1. The particulate lidar ratios at both 532 nm and 1064 nm are constant with respect to range (i.e., $S_{p,\lambda} = \sigma_{p,\lambda}(z) / \beta_{p,\lambda}(z)$).

2. The backscatter color ratio, χ, defined as the ratio of the particulate backscatter coefficients at the two wavelengths, is likewise range-invariant $\left(\text{i.e., } \chi = \beta_{p,1064}(z)/\beta_{p,532}(z)\right)$.

For elastic backscatter lidars, this first assumption is invoked in the majority of the published solutions for the lidar equation.[4,10,11] The second assumption can be shown to be equivalent to requiring a constant angstrom exponent throughout the layer, and the assumption of a constant angstrom coefficient is likewise well established in the literature (e.g., Voss et al.[12]) By applying this second assumption, this work develops a new two-color retrieval that, given a solution to the lidar equation at 532 nm, derives optimal estimates (in the least-squares sense) for the lidar ratio at 1064 nm and the backscatter color ratio.

The assumptions required here are essentially identical to those applied in the two-color algorithm initially developed by Potter[13] and subsequently expanded by Ackermann[14,15,16]. The Potter/Ackermann (P/A) approach assumes range invariant lidar ratios at both wavelengths, as in assumption 1 above, and a fixed linear relationship between the extinction coefficients in the scattering medium, such that $\alpha = \sigma_{p,1064}(z) / \sigma_{p,532}(z)$. Given the assumption of constant lidar ratios, the assumption of a constant backscatter color ratio is easily shown to be interchangeable with the original

Potter/Ackermann assumption: $\chi = \alpha \cdot (S_{532} / S_{1064})$. However, the algorithm described here frames the retrieval in a different context from the P/A technique. Apart from the solution mechanics, the main difference between the two algorithms is in the physical quantities that are assumed to be known prior to initiating the solution. These quantities in turn dictate the optical properties that are to be retrieved. In this paper I assume that an acceptable solution exists for the 532 nm measurements, and then derive S_{1064} and χ. In contrast, Ackermann's modification of the Potter algorithm assumes that both S_{532} and S_{1064} are known, and then extracts the extinction color ratio, α, and the layer two-way transmittance at the longer wavelength. This latter quantity is used as a boundary condition in a Klett retrieval;[17] the extinction profile at the shorter wavelength can then be obtained via the extinction color ratio.

Potter originally formulated his algorithm for a single component atmosphere. Because molecular contributions to the lidar signal were neglected, the lidar ratios at the two wavelengths could be absorbed into a constant term that cancels out in the subsequent mathematical manipulations. Lidar ratios therefore do not need to be known for the Potter algorithm to be successful. Unfortunately, the assumption of a single component atmosphere means that Potter's technique is not immediately applicable to a large number of real-world lidar signals.[1] In particular, Potter's algorithm cannot be applied reliably to the Nd:YAG wavelengths employed by space-based lidars. This limitation was later remedied by Ackermann, who derived the two-component analog to the Potter method. However, when expanding the technique to accommodate molecular scattering, Ackermann reintroduced the lidar ratios as a necessary part of the solution: Ackermann's algorithm requires both S_{532} and S_{1064} to be known (or specified) independently.

Ackermann's modification of the Potter algorithm can be considered as an optimization scheme that, for a given pair of lidar ratios, will determine the layer optical depth that satisfies a constant color ratio constraint. As in Ackermann, the algorithm introduced in this work assumes a two-component atmosphere; however, at most only one lidar ratio need be specified in advance. For retrievals applied to surface-attached aerosol layers, knowledge of the lidar ratio at the shorter wavelength is required, as is a near-range boundary condition for the particulate backscatter coefficient. For lofted layers, no a priori knowledge of either lidar ratio is required. The solution generated at the shorter wavelength (assumed here always to be 532 nm) is then combined with the assumed constant color ratio constraint in order to derive the lidar ratio at the second, longer wavelength (assumed here always to be 1064 nm). Section 2 of this paper begins with a brief review of standard techniques for deriving backscatter and extinction coefficients from lidar measurements, followed by the mathematical development of a two-color algorithm for retrieving the backscatter color ratio and lidar ratio at 1064 nm. Section 3 presents the results of numerical experiments designed to reveal the sensitivity of the method to errors in the various input parameters. The initial application of the algorithm to data acquired during the LITE mission is described in Section 4. Finally, Section 5 concludes with some discussion of future research and analysis that needs to be done to make the technique suitable for application to routine CALIPSO data processing.

2. MATHEMATICAL DERIVATION

2.1. Solution to the lidar equation

The initial framework for the algorithm is cast in terms of a multi-component equation describing the signal received by an elastic backscatter lidar:

$$P_\lambda(r) = \frac{C_\lambda}{r^2} \cdot \left(\beta_{m,\lambda}(r) + \beta_{p,\lambda}(r)\right) \cdot \exp\left(-2 \cdot \int_0^r \sigma_{m,\lambda}(r) + \sigma_{O_3,\lambda}(r) + \sigma_{p,\lambda}(r)\ dr\right) \quad (1)$$

The λ subscript indicates the laser wavelength, and the subscripts m, O_3, and p represent, respectively, molecular, ozone, and particulate components, where particulates are understood to include both clouds and aerosols. C_λ is the wavelength-specific lidar system constant, and is assumed to be known, albeit with some (presumably small) uncertainty. Assuming that $\beta_{m,\lambda}(r)$, $\sigma_{m,\lambda}(r)$, and $\sigma_{O3,\lambda}(r)$ are either known from meteorological data or well approximated by models, then

$$P_\lambda(r) = \frac{C_\lambda}{r^2} \cdot \left(\beta_{m,\lambda}(r) + \beta_{p,\lambda}(r)\right) \cdot T^2_{m,\lambda}(r) \cdot T^2_{O_3,\lambda}(r) \cdot \exp\left(-2 \cdot \int_0^r \sigma_{p,\lambda}(r)\ dr\right) \quad (2)$$

[1] It must be noted that Potter explored two-component solutions in an appendix included with his original article.

where

$$T^2_{k,\lambda}(r) = \exp\left(-2 \cdot \int_0^r \sigma_{k,\lambda}(r)\ dr \right). \tag{3}$$

Applying assumption 1 above, the particulate lidar ratio within the layer can now be defined as a range-invariant constant; that is

$$S_{p,\lambda} = \frac{\sigma_{p,\lambda}(r)}{\beta_{p,\lambda}(r)}. \tag{4}$$

The lidar equation can then be rearranged to derive the *particulate-attenuated total backscatter coefficient*, $B_\lambda(r)$, as follows:

$$B_\lambda(r) = \frac{r^2 \cdot P_\lambda(r)}{C_\lambda \cdot T^2_{m,\lambda}(r) \cdot T^2_{O_3,\lambda}(r)} = \left(\beta_{m,\lambda}(r) + \beta_{p,\lambda}(r)\right) \cdot \exp\left(-2 \cdot S_{p,\lambda} \cdot \int_0^r \beta_{p,\lambda}(r)\ dr \right). \tag{5}$$

In those cases where the lidar ratio is known, several standard methods are available to retrieve range-resolved profiles of particulate backscatter and extinction coefficients from equation (9). These include analytic solutions by Fernald et al.[10] and Klett[17] as well as numerical techniques such as those employed by Gambling and Bartusek[18] and others [11,19]. If the lidar ratio is not known, it can nonetheless be determined from the attenuated backscatter measurements provided that the lidar data can be augmented by a simultaneous measurement of the two-way transmittance over some range interval that includes the feature in question.[10] Unfortunately, for a variety of reasons, correlative measurements using other instruments such as radiometers are not universally available – as for example during LITE. However, as described earlier, for lofted layers the layer two-way transmittance can be obtained directly from the lidar data itself. The lidar ratio can then be retrieved directly from the measurement using analytical or iterative techniques. Methods for doing so are well documented in the current literature,[4,19,20] as are the requisite error analyses[21], and hence will not be reviewed here.

2.2. Adaptation for multiple scattering

Following Young[4], the effects of multiple scattering can be parameterized using a constant multiple scattering factor that modifies the particulate extinction coefficient. The particulate two-way transmittance term then becomes

$$T^2_{p,\lambda}(r) = \exp\left(-2 \cdot \eta_\lambda \cdot \int_0^r \sigma_{p,\lambda}(r)\ dr \right) \tag{6}$$

With this adaptation we can now rewrite equation (5) as

$$B_\lambda(r) = \left(\beta_{m,\lambda}(r) + \beta_{p,\lambda}(r)\right) \cdot \exp\left(-2 \cdot S'_{p,\lambda} \cdot \int_0^r \beta_{p,\lambda}(r)\ dr \right) \tag{7}$$

where $S'_{p,\lambda} = \eta_\lambda \cdot S_{p,\lambda}$ is the *effective lidar ratio*. Although S and S′ have very different physical interpretations, in the formulation presented here they are mathematically interchangeable and therefore algorithms capable of retrieving S can likewise retrieve S′ with equal ease.

2.3. Deriving the backscatter color ratio and the effective lidar ratio at 1064 nm

Let us assume that one of the aforementioned techniques for retrieving lidar ratio and a profile of backscatter coefficients has been successfully applied to a lofted layer measured at 532 nm. We can then apply assumption 2 above to insert a pair of variable substitutions into the 1064 nm lidar equation that will allow us to retrieve a best fit solution for the backscatter color ratio, χ, and the 1064 nm lidar ratio, S_{1064}. Using assumption 2, the particulate backscatter and extinction coefficients at 1064 nm can be written in terms of their 532 nm analogs as follows:

$$\beta_{p,1064}(z) = \chi \cdot \beta_{p,532}(z) \tag{8a}$$

$$\sigma_{p,1064}(r) = S_{p,1064} \cdot \beta_{p,1064}(r) = \chi \cdot S_{p,1064} \cdot \beta_{p,532}(r) \tag{8b}$$

Substituting (8) into (5) yields

$$B_{1064}(r) = \left(\beta_{m,1064}(r) + \chi \cdot \beta_{p,532}(r)\right) \cdot \exp\left(-2 \cdot \chi \cdot S_{p,1064} \cdot \int_0^r \beta_{p,532}(r')\ dr'\right) \tag{9}$$

Alternately, setting $\gamma_{p,532}(r) = \int_0^r \beta_{p,532}(r')\ dr'$ we can write

$$B_{1064}(r) = \left(\beta_{m,1064}(r) + \chi \cdot \beta_{p,532}(r)\right) \cdot \exp\left(-2 \cdot \chi \cdot S_{p,1064} \cdot \gamma_{p,532}(r)\right) \tag{10}$$

Examining the range-dependent components of equation (10), we see that $B_{1064}(r)$ is a known measurement, $\beta_{m,1064}(r)$ is assumed to be known from meteorological data or models, and, because we have previously obtained a solution at 532 nm, $\beta_{p,532}(r)$ and $\gamma_{p,532}(r)$ are likewise known values. The only unknown values in equation (10) are thus the range-invariant quantities χ and $S_{p,1064}$. Therefore, assuming the layer thickness spans two or more range bins, the measurements of $B_{1064}(r)$ can be seen as representing a system of equations in the unknowns χ and $S_{p,1064}$. A solution for this system can be derived via the method of least squares; that is, we seek the minimum of a function $F(\chi, S_{p,1064})$ where

$$F(\chi, S_{p,1064}) = \frac{1}{2} \cdot \sum_{k=\text{layer top}}^{\text{layer base}} \left(\left(\beta_{m,1064}(r_k) + \chi \cdot \beta_{p,532}(r_k)\right) \cdot \exp\left(-2 \cdot \chi \cdot S_{p,1064} \cdot \gamma_{p,532}(r_k)\right) - B_{1064}(r_k)\right)^2 . \tag{11}$$

Estimates for χ and $S_{p,1064}$ can be derived from equation (11) by applying standard techniques for the numerical solution of nonlinear least squares problems (see, for example, the text by Dennis and Schnabel[22]).

3. SENSITIVITY ANALYSES

The general error analysis for nonlinear least squares problems can be notoriously intractable. Error estimates for a specific solution can be derived from the final approximation to the Hessian matrix generated by the nonlinear least squares solver.[23] However, a more intuitive understanding of the global correlations between input uncertainties and output errors is often best obtained by numerical experiments, and that is the approach taken here. A simulation study was designed to analyze a sequence of uniform and homogeneous layers embedded in an otherwise pure molecular atmosphere. Based on the author's previous experience with similar retrieval schemes, the dominant sources of output errors are expected to arise from (1) errors in the solution obtained at 532 nm, (2) the signal-to-noise ratio (SNR) of the 1064 nm backscatter measurement, and (3) uncertainties in 1064 nm calibration and background subtraction. (Note that uncertainties due to the 532 nm SNR, calibration, and background subtraction are all reflected in the errors ascribed to the 532 nm backscatter solution.) The current work describes results obtained from a series of numerical experiments that address the first two of these three categories. The effects of 1064 nm calibration uncertainties will be investigated in the future, but are not considered at present.

The simulated data used in this study consists of a single layer embedded in an otherwise clean molecular atmosphere. Each layer was assigned a top altitude at 2.52 km, a base altitude at 0.51 km, and was modeled as a having a uniform distribution of extinction coefficients with a layer optical depth of 0.255 at 532 nm (i.e., $\sigma_{P,532}(z) = 0.125\ km^{-1}$ for all z within the layer). The vertical resolution of the simulated data is 30 meters. Five different layer types were tested. These included a water cloud and four distinct aerosol types. The intrinsic scattering properties of the aerosol layers varied according to a set of models derived from AERONET measurements.[24] The intrinsic and extrinsic scattering properties for all models are listed below in Table 1.

Table 1: Intrinsic and extrinsic scattering properties of the cloud and aerosol models used in the simulation study. The base and top altitudes are identical for all layers tested, as are the layer optical depths.

Feature Type	S_{532} (sr)	S_{1064} (sr)	χ	α	$\beta_{P,532}$ ($km^{-1}sr^{-1}$)	$\beta_{P,1064}$ ($km^{-1}sr^{-1}$)
Water Cloud (sr)	18.00	18.00	1.00	1.00	0.00694	0.00694
Desert Dust	36.39	27.97	0.79	0.61	0.00344	0.00271
Polluted Dust	62.35	29.52	1.07	0.51	0.00200	0.00213
Biomass Burning	68.11	37.12	0.68	0.37	0.00184	0.00124
Polluted Continental Aerosol	69.45	29.47	0.72	0.31	0.00180	0.00130

For all profiles analyzed, realistic noise levels consistent with those measured during the LITE mission were introduced via a Poisson-distributed random number generator. The noise levels were scaled according to the expected backscatter intensity of each feature type, so that the SNR for a strongly backscattering feature such as a water cloud would be greater than the SNR for a weakly backscattering feature such as a biomass burning plume. Additional errors in the 532 nm solutions were introduced by adjusting the lidar ratio used to generate the input backscatter coefficients. For each feature type the lidar ratio was varied by ±30% from the true lidar ratio in increments of 10%. Twenty individual profiles were tested at each lidar ratio increment, so that for each feature type a total of one hundred and forty simulated profiles were generated and solved. Figure 2 shows an example of a pair of profiles used during the tests of 532 nm input errors. For this example, the SNR within the feature is 52.3 at 532 nm and 30.9 at 1064 nm. These values are roughly equivalent to those that would be expected from a 40-km horizontal average of LITE data. Errors due solely to SNR were investigated by directly manipulating the SNR of the input profiles via an arbitrarily specified gain constant, a procedure that is functionally equivalent to increasing (or decreasing) the amount of horizontal averaging done prior to analyzing a given set of measurements. The profiles used in the SNR-only testing are similar in all respects to those shown in Figure 2, except that the noise level varied from the equivalent of 1-km of horizontal averaging (3 LITE laser pulses, 532 nm SNR ~8) to 80-km of horizontal averaging (240 pulses, 532 nm SNR ~75). For the SNR-only testing, solutions were generated for 40 unique profiles at each discrete SNR level. The 532 nm lidar ratios used in this phase of the testing were error free; however, due to the noise in the simulated 532 nm signal, the 532 nm backscatter solutions – i.e., $\beta_{p,532}(z)$ and its integral, $\gamma_{p,532}(z)$ – were contaminated with random error commensurate with the specified 532 nm SNR.

Figure 2: Test input profiles showing simulations of desert dust at 532 nm (left, in green) and 1064 nm (right, in red). The in-feature SNR (i.e., computed between 2.52-km and 0.51-km) is 52.3 for the 532 nm channel and 30.9 for the 1064 channel, and is equivalent to what would be expected from 40-km horizontal averages of LITE measurements.

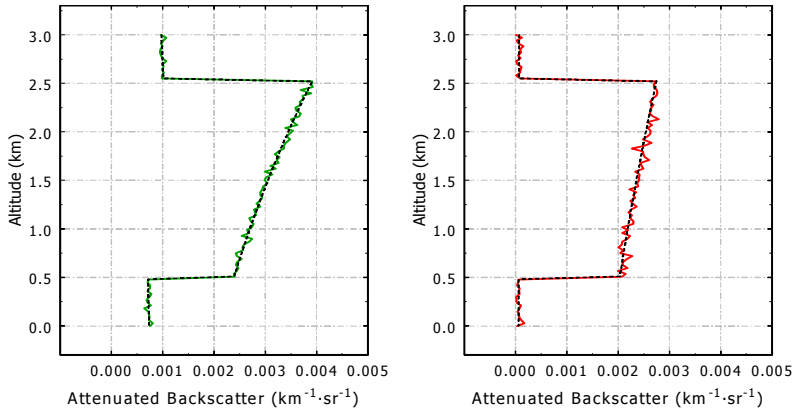

The influence of the SNR of the measurements on the derived solutions for all models is presented in Figure 3. On a log-log scale, the relative error or "noise-to-signal ratio" of the output – that is, the standard deviation of the retrieved values with respect to the target value, normalized by the target value – is seen to vary in an approximately linear fashion with respect to the SNR of the lidar signal for both lidar ratio (left panel of Figure 3) and color ratio (right panel). Not surprisingly, the amount of averaging required to obtain S_{1064} uncertainties of 10% or less is seen to be related to the magnitude of the backscatter coefficients and/or the extinction color ratio (see columns 5, 6, and 7 in Table 1).

Figure 3: Influence of SNR on derived values for 1064 nm lidar ratio and backscatter color ratio for uniform layers having an optical depth of 0.255 . The x-axis 532 nm SNR values correspond to horizontal averages of LITE data over 1, 2, 5, 10, 20, and 80 kilometers.

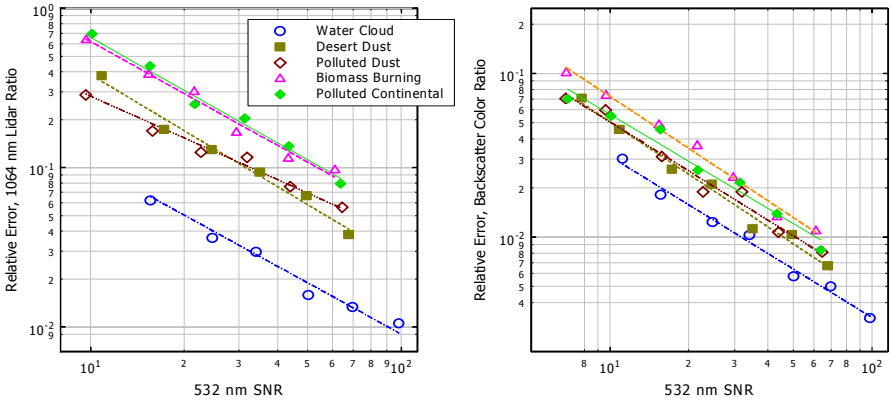

Figure 4 shows the composite results obtained from the 532 nm input errors tests. In the left-hand panel, relative errors in S_{1064}, $\Delta S_{relative} = (S_{measured} - S_{true})/S_{true}$, are shown as a function of the (specified) relative errors in S_{532}. Relative errors in χ are shown in the right-hand panel. Individual data points represent the average solution obtained from a sequence of 20 independently generated profiles; the error bars represent one standard deviation about the mean solution. In both cases, the relative error introduced into the retrieved parameters as a result of an incorrect solution at 532 nm is well represented by a linear function of the relative error in the 532 nm lidar ratio. Also in both cases, the magnitude of the relative error varies differently according to the individual scattering species. The perturbations are surprisingly small for the backscatter color ratio. Even for the most sensitive aerosol models (biomass burning and polluted continental), the errors in the retrieved color ratios were approximately 2.5% ± 1.5% for an input error of 30%. From Figure 3 we see that the expected uncertainties at this SNR are in the range of 1.5% for both the biomass burning and polluted continental models, and can therefore conclude that the retrieval of the backscatter color ratio is relatively insensitive to errors in the lidar ratio used to generate the 532 nm solution.

Figure 4: Relative errors in S_{1064} (left panel) and χ (right panel) as a function of relative errors in S_{532}; the slope of the linear regression line, m, for each test case is given in the legend.

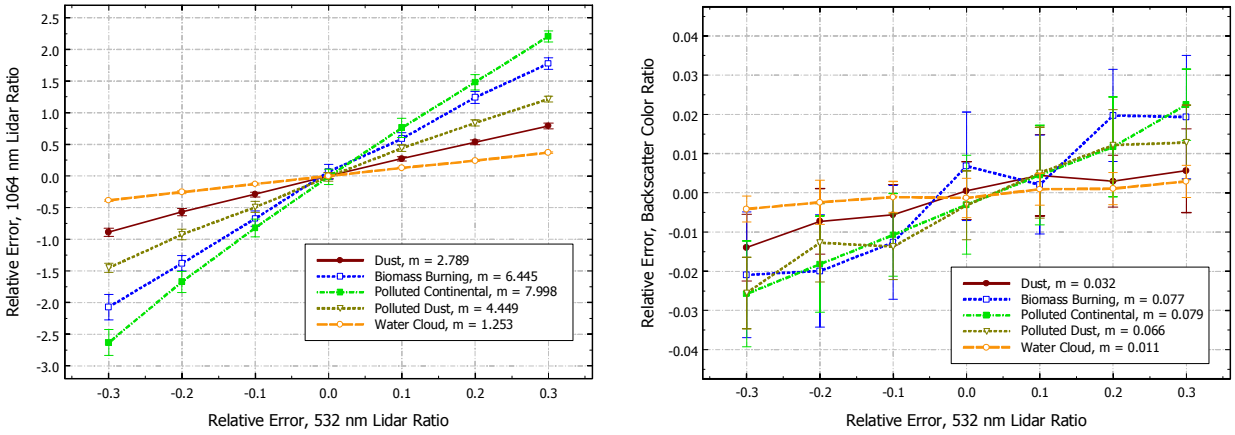

Regrettably (but not surprisingly), this insensitivity does not extend to the retrievals of the 1064 nm lidar ratio. The errors in the retrieved value of S_{1064} as a function of S_{532} error are substantially larger than the corresponding color ratio errors, and vary from an approximately 1:1 output-to-input relationship for water clouds to as much as 8:1 for the polluted continental aerosol model. (By contrast, the maximum color ratio error slope is roughly two orders of magnitude smaller, on the order of 0.08:1.) The exact cause for the difference in error propagation with respect to scattering species is not yet firmly established. It is however quite obvious that the 532 nm lidar ratio must be

reasonably well known in order to retrieve acceptably accurate values for the 1064 nm lidar ratio when applying this technique to particulates with a low extinction color ratios.

4. APPLICATION TO LITE DATA

The method described above has been applied to two specific regions of LITE data: cirrus cloud data obtained during orbit 23 and lofted aerosol data acquired during orbit 83. This section presents the results of both analyses.

4.1. Retrievals of cloud parameters

The cirrus cloud data, shown below in Figure 5, was acquired during an overpass of the Caribbean Sea on orbit 23, and was taken from a period of nighttime low gain operation. During LITE, high gain nighttime measurements of clouds with moderate optical depths were very frequently contaminated by saturated signals, and so while an estimate of the two-way transmittance is easily retrieved from the molecular return beneath a cloud, the remainder of the analysis cannot be carried out because the backscatter measurements are truncated at the upper limit of the LITE digitizers. Low gain data from orbits 23, 24, and 27 present the best opportunity for analyzing an uninterrupted sequence of cloud profiles for which the clouds are both transmissive and unsaturated. (The implications of this choice are explored further in Appendix A.)

Prior to processing, all data was averaged to a 10-km horizontal resolution. The data within the cloud was further averaged to a 150 meter vertical resolution. Data outside the cloud boundaries was averaged to a vertical resolution of 300 meters. The vertical lines shown in the image represent the 10-km segment boundaries. For this initial analysis, segments containing broken cloud (i.e., those segments between samples 5 and 6) were not processed. The constraint required for the 532 nm lidar ratio retrieval was obtained by measuring the cloud two-way transmittance in the clear air region between 10.5-km and 4.5-km beneath each cloud. The mean cloud optical depth derived in this manner is 0.20 ± 0.05. The 532 nm in-cloud SNR within each segment is estimated to vary between 64 and 80, depending on the magnitude of the backscatter intensity. The uncertainties in the effective lidar ratios retrieved at 532 nm are estimated to be in the range of ±17%.

Figure 5: Left panel: LITE attenuated scattering ratios acquired during orbit 23 at 532 nm; right panel: lidar ratios and backscatter color ratio retrieved for each cloud segment.

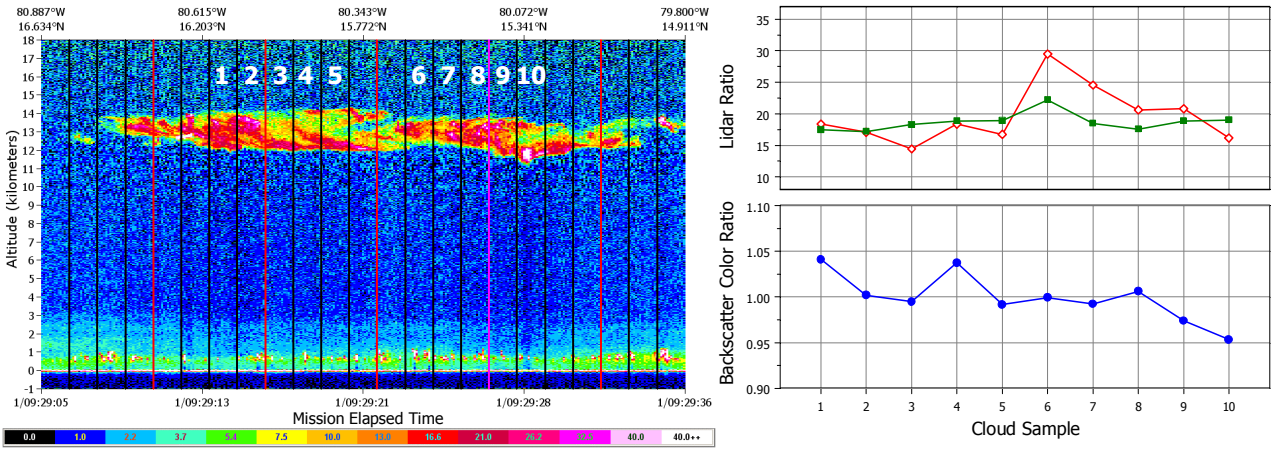

Retrieval statistics for each cloud segment are show in Table 2. Relative error estimates for S_{1064} and χ are computed as the root-sum-square of the individual error contributions from SNR and 532 nm lidar ratio uncertainties; that is,

$$e_{\text{relative}} = \sqrt{\left(10^{m_{SNR}\cdot\log_{10}(SNR_{532})+b_{SNR}}\right)^2 + \left(m_S\cdot\Delta S_{532} + b_S\right)^2} \qquad (12)$$

where m_{SNR} is the slope of the relative error with respect to the measured SNR at 532 nm (see Figure 3), m_S is the slope of the relative error with respect to lidar ratio error, b_{SNR} and b_S are the corresponding intercepts of the linear fits, and ΔS_{532} is the estimated error in the lidar ratio retrieval at 532 nm. For this set of statistics, errors due to lidar ratio uncertainty were approximated using the water cloud model. Optical depth at 1064 nm (τ_{1064}) is derived using the

retrieved value of S_{1064}. Column averages are given in the bottom row. Note that if we assume that the lidar ratio remains constant over the entire 120 km spanned by the ten samples analyzed, then the most probable value of the mean is computed by a weighted average, with the weights in each case being equal to the estimated variance.[23] Under this assumption the intrinsic scattering properties of this particular cloud are $S_{532} = 18.42 \pm 0.93$; $S_{1064} = 17.78 \pm 1.14$; and $\chi = 1.00 \pm 0.002$.

Table 2: Retrieval statistics for the cloud data shown in Figure 5

	top	base	SNR	τ_{532}	S_{532}	ΔS_{532}	τ_{1064}	S_{1064}	ΔS_{1064}	χ	$\Delta\chi$
1	14.22	11.82	78.4	0.24	17.47	2.47	0.27	18.35	3.27	1.04	0.01
2	14.22	11.82	80.3	0.25	17.18	2.52	0.25	17.07	3.15	1.00	0.01
3	14.22	11.82	65.0	0.16	18.29	2.98	0.13	14.43	2.96	1.00	0.01
4	14.22	11.82	68.1	0.19	18.85	2.91	0.19	18.35	3.57	1.03	0.01
5	14.22	11.82	66.0	0.17	18.90	3.98	0.15	16.74	4.43	0.99	0.01
6	13.92	11.97	63.5	0.15	22.22	4.42	0.20	29.49	7.37	1.00	0.01
7	13.92	11.97	68.4	0.14	18.48	3.86	0.19	24.55	6.45	0.99	0.01
8	13.92	11.97	78.2	0.19	17.58	3.23	0.23	20.61	4.76	1.01	0.01
9	13.92	11.37	73.2	0.25	18.85	2.88	0.28	20.79	4.01	0.97	0.01
10	13.77	11.07	72.0	0.28	19.01	2.21	0.23	16.16	2.38	0.95	0.00
Avg	14.06	11.74	71.3	0.20	18.68	3.15	0.21	19.65	4.24	1.00	0.01

4.2. Retrievals of aerosol parameters

The aerosol data, shown below in Figure 6, was taken from an extended measurement of lofted Saharan dust acquired off the coast of Western Sahara during LITE orbit 83. Due to the limited spatial region available for obtaining the necessary attenuation constraint at 532 nm, for this retrieval all data was averaged to a resolution of 20-km horizontally and 75 meters vertically. The constraint required for the 532 nm lidar ratio retrieval was obtained by measuring the layer attenuation over the entire clear air region between the base of the lofted aerosol layer and the top of the heterogeneous cloud and aerosol layer below. The mean aerosol optical depth derived in this manner is 0.16 ± 0.03. The 532 nm SNR within the layer boundaries is estimated to vary between 44 and 49. The uncertainties in the effective lidar ratios retrieved at 532 nm are estimated to be in the range of ±18.5%.

Figure 6: Right panel: LITE attenuated scattering ratios acquired during orbit 83 at 532 nm; left panel: lidar ratios and backscatter color ratio retrieved for each aerosol segment.

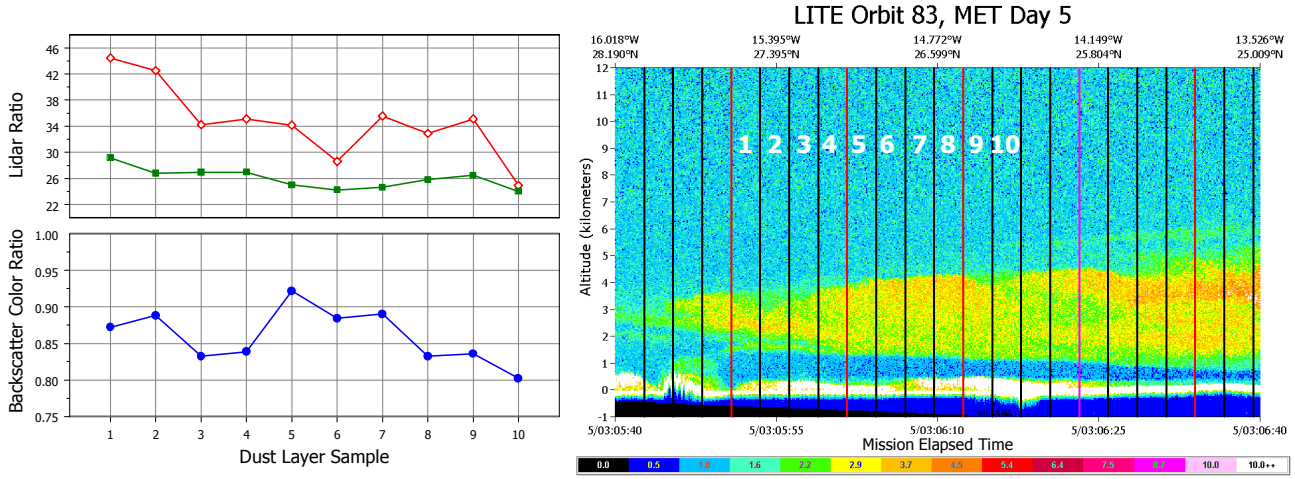

Retrieval statistics for the desert dust data are shown in Table 3. Optical depth at 1064 nm and error estimates for S_{1064} and χ are computed in the same manner as for the cloud data, except that for the dust data error propagation due to lidar ratio uncertainties was approximated using the simulation results from the desert dust model; i.e.,

$$\Delta S_{1064} = \sqrt{0.062^2 + \left(2.789 \cdot \Delta S_{532}\right)^2} \text{ and } \Delta\chi = \sqrt{0.010^2 + \left(0.032 \cdot \Delta S_{532}\right)^2}$$

where the first term under the each radical quantifies SNR effects and the second term represents the contributions from lidar ratio uncertainties. Assuming once again that the lidar ratios remain constant over the entire 200 km spanned by the ten samples analyzed, the intrinsic scattering properties characterizing this dust event are S_{532} = 25.73 ± 1.43; S_{1064} = 33.13 ± 5.20; and χ = 0.86 ± 0.003.

Table 3: Retrieval statistics for the desert dust data shown in Figure 6

	top	base	SNR	τ_{532}	S_{532}	ΔS_{532}	τ_{1064}	S_{1064}	ΔS_{1064}	χ	$\Delta\chi$
1	4.06	1.29	44.3	0.11	29.17	7.57	0.14	44.47	32.32	0.87	0.01
2	4.29	1.29	44.5	0.11	26.79	6.27	0.15	42.52	27.86	0.89	0.01
3	4.36	1.21	46.8	0.14	26.94	5.17	0.15	34.23	18.44	0.83	0.01
4	4.29	1.21	49.0	0.17	26.97	4.05	0.18	35.13	14.86	0.84	0.01
5	4.81	1.21	48.1	0.17	25.00	4.25	0.21	34.15	16.31	0.92	0.01
6	4.81	1.14	48.7	0.17	24.24	4.66	0.18	28.59	15.43	0.88	0.01
7	4.81	1.14	49.4	0.19	24.64	3.63	0.24	35.57	14.79	0.89	0.01
8	4.96	1.06	48.0	0.19	25.81	3.69	0.20	32.88	13.26	0.83	0.01
9	4.81	1.06	47.3	0.18	26.46	4.06	0.20	35.11	15.18	0.84	0.01
10	4.89	0.99	46.9	0.16	24.02	5.02	0.13	24.92	14.60	0.80	0.01
Avg	4.61	1.16	47.3	0.16	26.00	4.84	0.18	34.76	18.31	0.86	0.01

A word of caution is in order here. The error estimates given above may be unduly pessimistic, as the CALIPSO dust model used in the sensitivity analyses is not an especially good fit for the actual measured data. Due to multiple scattering effects, the lidar ratios derived from LITE data must be considered to be *effective* lidar ratios (i.e., $S' = \eta \cdot S$), as opposed to the single scattering lidar ratios specified in Table 1. Therefore the fact that the 532 nm lidar ratio is lower than the model value is in general to be expected, as $\eta \leq 1$. However, the fact that S_{1064} is larger than S_{532} is somewhat more interesting, as this fact is at odds with the AERONET-derived dust model. At present no definitive explanation for this phenomenon is offered. (It should be noted though that Mie calculations applied to bimodal size distributions can produce similar results.) With respect to error propagation, simulated retrievals for a configuration of optical properties identical to the average values reported above for the LITE dust data shows that the slope of the relative errors in S_{1064} as a function of errors in S_{532} is flatter by a factor of greater 2 when compared to the slope of the dust model simulations (1.19 vs. 2.79). It is therefore likely that the error estimates given above overstate the actual error in the retrieved parameters.

5. DISCUSSION AND CONCLUSIONS

In this paper I have presented a new algorithm for retrieving lidar ratios at 1064 nm from backscatter lidar data. Initial simulation studies show the retrieval of S_{1064} to be sensitive to the particle type being measured: retrievals in layers with high extinction color ratios appear to be much more sensitive to errors in S_{532} than do retrievals in layers with lower α values. The second parameter simultaneously retrieved by this algorithm, the backscatter color ratio, is more resilient, and can be retrieved with excellent accuracy even in noisy data and/or when the lidar ratio at 532 is poorly known.

Future work will investigate such issues as (a) sensitivities to uncertainties in the 1064 nm calibration constant; (b) relative sensitivity issues with respect to the detectors and SNR; (c) errors induced due to feature optical depths (e.g., how do the error slopes shown in Figure 4 change as the measured optical depths grow larger or smaller); and (d) the application of more robust numerical methods (e.g., orthogonal distance regression[25]).

APPENDIX A: A NOTE ABOUT THE CALIBRATION OF THE LITE 1064 nm DATA

For this study, the calibration of the LITE 1064 data was done using the CALIPSO cirrus cloud technique reported in Reagan, Wang, and Osborn.[26] This technique assumes that the scattering from robust clouds is spectrally independent in the 532-to-1064 nm range. With respect to the current work, the significance of this assumption is that for clouds in

the calibration region, both the backscatter and extinction color ratios are defined to be 1.00, and the 1064 nm calibration constant is adjusted to enforce this condition.

Since a color ratio of 1.00 is mandated by the calibration process, retrieval of a value very close to 1.00 is to be expected: retrieving a value other than ~1.00 would suggest flaws in the method concept or the analysis codes. The cirrus cloud results reported here should therefore be viewed solely from the perspective of algorithm performance. However, this proviso applies only to the backscatter color ratios and 1064 nm lidar ratios; the effective lidar ratios at 532 were obtained using the independently derived calibration constants recorded in the LITE Level 1 data[27]. Also, it should be noted that specific cloud deck used in this study was not included in the calibration calculations of Reagan et al.

The calibration ratio, C_{1064} / C_{532}, used in the aerosol analysis is identical to that used in the cloud analysis. Both sets of calculations used a calibration ratio of 88.

REFERENCES

1. D. M. Winker, R. H. Couch, and M. P. McCormick, "An overview of LITE: NASA's Lidar In-space Technology Experiment", *Proc. IEEE 84*, pp. 164-180, Feb. 1996.
2. J. D. Spinhirne and S. P. Palm, "Space based atmospheric measurements by GLAS", *Selected papers of the 18th International Laser Radar Conference (ILRC)*, Springer-Verlag, Berlin, pp. 213-216, 1996.
3. D. M. Winker, J. Pelon, and M. P. McCormick, "The CALIPSO mission: Spaceborne lidar for observation of aerosols and clouds", Proc. SPIE, **4893**, pp. 1-11, 2002.
4. S. A. Young, "Analysis of lidar backscatter profiles in optically thin clouds", Appl. Opt. **34**, pp. 7019-7031, 1995.
5. A. H. Omar, D. M. Winker, J.-G. Won, M. A. Vaughan, C. A. Hostetler, and J. A. Reagan, "Selection Algorithm for the CALIPSO Lidar Aerosol Extinction-to-Backscatter Ratio", Proc. IEEE, International Geoscience and Remote Sensing Symposium, 2003 (in press)
6. S. Palm, W. Hart, D. Hlavka, E. J. Welton, A. Mahesh, and J. Spinhirne, "Geoscience Laser Altimeter System (GLAS) Algorithm Theoretical Basis Document Version 4.2, GLAS Atmospheric Data Products", available on-line at http://eospso.gsfc.nasa.gov/eos_homepage/for_scientists/atbd/docs/GLAS/ATBD-GLAS-01.pdf.
7. G. Pappalardo, J. Bösenberg, D. Balis, A. Boselli, L. Komguem, G. Larchevêque, V. Matthias, L. Mona, I. Mattis, A. Papayannis, M. R. Perrone, and V. Rizi, "EARLINET measurements of the aerosol extinction-to-backscatter ratio", *Lidar Remote Sensing in Atmospheric and Earth Sciences: Reviewed and Revised Papers Presented at the 21st International Laser Radar Conference (ILRC)*, L. Bissonnette, G. Roy, and Gilles Vallée, eds., Quebec, Canada, pp. 301-304, 2002.
8. R. A. Ferrare, D. D. Turner, L. A. Heilman, O. Dubovik, T. P. Tooman, and W. F. Feltz, "Raman lidar measurements of the aerosol extinction-to-backscatter ratio over the Southern Great Plains", *J. Geophys. Res.*, **106**, No. D17, pp. 20,333-20,348, 2001.
9. S. J. Masonis, *An empirical study of the lidar ratio and its variability, with implications for determining climate forcing by satellite-borne lidar*, Ph.D. dissertation, University of Washington, 257 pp., 2001 [Available from Bell and Howell Information and Learning, 300 North Zeeb Road., P.O. Box 1346, Ann Arbor, MI 48106-1346]
10. F. G. Fernald, B. M. Herman, and J. A. Reagan, "Determination of Aerosol Height Distributions by Lidar", *J. Appl. Meteor.*, **11**, pp. 482-489, 1972.
11. C. M. R. Platt, "Lidar and radiometric observations of cirrus clouds", *J. Atmos. Sci.*, **30**, pp. 1191-1204, 1973.
12. K. J. Voss, E. J. Welton, P. K. Quinn, R. Frouin, M. Miller, and R. M. Reynolds, "Aerosol optical depth measurements during the Aerosols99 experiment" , *J. Geophys. Res.*, **106**, No. D18, pp. 20,811-20,819, 2001.
13. J. F. Potter, "Two-frequency lidar inversion technique", *Appl. Opt.*, **26**, pp. 1250-1256, 1987.
14. J. Ackermann, "Two-wavelength lidar inversion algorithm for a two-component atmosphere", *Appl. Opt.*, **36**, pp. 5134-5143, 1997.
15. J. Ackermann, "Two-wavelength lidar inversion algorithm for a two-component atmosphere with variable extinction-to-backscatter ratios", *Appl. Opt.*, **37**, pp. 3164-3171, 1998.
16. J. Ackermann, "Analytical solution of the two-frequency lidar inversion technique", *Appl. Opt.*, **38**, pp. 7414-7418, 1999.
17. J. D. Klett, "Lidar inversion with variable backscatter/extinction ratios", *Appl. Opt.*, **24**, pp. 1638-1643, 1985.

18. D. J. Gambling and K. Bartusek, "Lidar observations of tropospheric aerosols", *Atmos. Environ.*, **6**, pp. 181-190, 1972.
19. J. M. Alvarez and M. A. Vaughan, "Numerical calculation of cloud optical extinction from lidar", *OSA Proceedings on the Inaugural Forum for the Research Center for Optical Physics*, **19**, pp. 90-95, Arlene Maclin, Ed.; Optical Society of America, Washington, D.C., 1994.
20. C. Mitrescu and G. L. Stephens, "A New Method for Determining Cloud Transmittance and Optical Depth Using the ARM Micropulsed Lidar", *J. Atmos. Ocean. Tech.*, **19**, pp. 1073-1081, 2002.
21. M. Del Guasta, "Errors in the retrieval of thin-cloud optical parameters obtained with a two-boundary algorithm", *Appl. Opt.*, 37, pp. 5522-5540, 1998.
22. J. E. Dennis and R. B. Schnabel, *Numerical Methods for Unconstrained Optimization and Nonlinear Equations*, Society for Industrial and Applied Mathematics (SIAM), Philadelphia, 1996.
23. P. R. Bevington and D. K. Robinson, *Data Reduction and Error Analysis for the Physical Sciences*, McGraw-Hill, New York, 1992.
24. A. H. Omar, J.-G. Won, Sun-Chang Yoon, and M. P. McCormick, "Estimation of Aerosol Extinction-to-Backscatter Ratios using AERONET Measurements and Cluster Analysis", *Lidar Remote Sensing in Atmospheric and Earth Sciences: Reviewed and Revised Papers Presented at the 21st International Laser Radar Conference (ILRC)*, L. Bissonnette, G. Roy, and Gilles Vallée, eds., Quebec, Canada, pp. 373-376, 2002.
25. P. T. Boggs, R. H. Byrd, J. E. Rogers, and R. B. Schnabel, *User's Reference Guide for ODRPACK Version 2.01 – Software for Weighted Orthogonal Distance Regression*, NISTIR 92-4834, U. S. Department of Commerce, National Institute of Standards and Technology, Gaithersburg, MD 20899 (also available electronically via NetLib at http://www.netlib.org/odrpack/).
26. J. A. Reagan, X. Wang, and M. T. Osborn, "Spaceborne Lidar Calibration From Cirrus and Molecular Backscatter Returns", *IEEE T. Geosci. Remote.*, **40**, No. 10, pp. 2285-2290, 2002.
27. M. T. Osborn, "Calibration of LITE data", *ILRC 19th International Laser Radar Conference*, U. Singh, S. Ismail, and G. Schwemmer, eds., NASA/CP-1998-207671/PT1, pp. 245-247, 1998 (addition information is available at the LITE web site; see http://www-lite.larc.nasa.gov/calibration/calibration.html).